Distinct Phototrophic Community Structure on a Central Asian Glacier: Predominance of Filamentous Cyanobacteria and Absence of Glacier Algae (*Ancylonema* spp.)

Yunjie Chen[1,2], Nozomu Takeuchi[3*], Sota Tanaka[3], Saifei Li[1], Weizhen Zhang[1], Xingyu Huang[4], and Zhongqin Li[5]

[1]Center for Pan-Third Pole Environment, Lanzhou University, Lanzhou, China
[2]Chayu Integrated Observation and Research Station of the Xizang Autonomous Region, Xizang, China
[3]Center for Environmental Remote Sensing, Chiba University, Chiba, Japan
[4]Institute of Tibetan Plateau Research, Chinese Academy of Sciences, Beijing, China
[5]State Key Laboratory of Cryospheric Sciences/Tien Shan Glaciological Station, Northwest Institute of Eco-Environment and Resources, Chinese Academy of Sciences, Lanzhou, China

Correspondence to: Nozomu Takeuchi (ntakeuch@faculty.chiba-u.jp)

Abstract. Cold-adapted algae and cyanobacteria are key drivers of snow and ice albedo reduction, yet their dynamics on dust-rich Central Asian glaciers remain poorly understood compared to the well-documented algal blooms in the Arctic. This study investigated the spatio-temporal distribution of phototrophic communities on Urumqi Glacier No.1, eastern Tien Shan, during a two-month melt season. Our findings reveal a distinct seasonal succession where snow-covered surfaces were dominated by snow algae *Chloromonadinia* species, whereas the ablation of snow exposed the bare-ice surface, manifesting as a sharp biomass increase dominated by the newly uncovered filamentous cyanobacteria (Oscillatoriaceae). Notably, glacier algae such as *Ancylonema* spp., which drive darkening on Arctic ice, were entirely absent, suggesting a fundamental ecological divergence. Statistical analyses indicated that cyanobacterial proliferation is closely linked to environmental factors, showing significant positive correlations with mineral-derived ions and negative correlations with inorganic nitrogen. These results, supported by recent evidence that specialized cyanobacterial taxa drive the initiation and structural development of cryoconite granules, suggest that mineral-rich glacier surfaces may provide environmental conditions favorable for the persistence of cyanobacteria-dominated communities. The widespread coverage of bare ice surfaces by dispersed cryoconite composed of filamentous cyanobacteria and mineral particles may contribute to sustained biological darkening throughout the melt season, contrasting with the transient snow algal blooms

commonly observed in polar regions. Our study highlights the necessity of integrating region-specific microbial dynamics, which is characterized by the absence of glacier algae and the dominance of mineral-buffered cyanobacterial communities, into glacier mass balance models to improve the accuracy of future projections for Central Asian water resources.

1 Introduction

Glacier and ice sheet constitute a distinct microbe-dominated biome within the Earth system (Anesio and Laybourn-Parry, 2012), harboring up to 10^{29} microbial cells (Irvine-Fynn and Edwards, 2014). The presence of liquid water, which is primarily from surface meltwater during the summer melt season, is one of key limiting factors for microbial activity (Hodson et al., 2008). Seasonal melting transforms glacier surfaces from a snow-covered landscape in winter to a mosaic of habitats in summer, with bare ice prevailing in the ablation zones and snowpack persisting in high-elevation accumulation zones (Stibal et al., 2012a). These snow and bare-ice habitats differ markedly in their physical and chemical properties, leading to distinct microbial communities (Yoshimura et al., 1997; Lutz et al., 2017). However, due to accelerated global glacier shrinkage (Hugonnet et al., 2021), the spatial extent of microbial habitats on glacier and ice sheet surfaces is rapidly diminishing. Therefore, investigating the spatial distribution and abundance of microbial taxa across icy environments is not only critical for understanding the ecological dynamics of glacier surface communities, but also for preserving a biological signature of these unique and increasingly vulnerable ecosystems.

Algae and cyanobacteria are key cold-adapted photosynthetic microorganisms that play a dominant role on biological carbon accumulation on glacier surfaces during melt season (Anesio et al., 2017). For example, eukaryotic green algae contribute up to 97% of the total photoautotrophic carbon fixation on the surface of the Greenland Ice Sheet (Yallop et al., 2012). Cyanobacteria are the primary contributors to photosynthetic activity, accounting for approximately 75%–93% of carbon fixation within the cryoconite hole on Werenskioldbreen glacier in Svalbard (Stibal and Tranter, 2007).

In addition to their role in carbon cycling, these microorganisms contribute to the acceleration of snow and ice melt by reducing surface albedo. Pigmented algae, can proliferate during the melt season, leading to visible algal blooms that darken the surface of snow and ice of ice sheet and glacier environments and enhance solar radiation absorption (Williamson et al., 2018; Takeuchi, 2013).

Filamentous cyanobacteria produce extracellular polymeric substances (EPS) that facilitate the aggregation of mineral particles, forming dark-colored cryoconite granules (Stibal et al., 2012b; Anesio et al., 2017; Landford et al., 2010), which further lower surface albedo and enhance localized melting on glacier surfaces (Cook et al., 2016; Kohshima et al., 1993; Takeuchi et al., 2018).

The habitats of algae and cyanobacteria on glacier surfaces are heterogeneous. In cryoconite granules and cryoconite holes on ablation surfaces, filamentous cyanobacteria, particularly members of the order Oscillatoriales, such as *Phormidesmis priestleyi*, *Phormidium* sp., and *Leptolyngbya* sp., are typically dominant and play a crucial role in formation of cryoconite granules (Singh et al., 2021; Segawa et al., 2017; Uetake et al., 2019). On glacier ice surface, algae from the order Zygnematales, including *Ancylonema nordenskiöldii*, *Ancylonema alaskanum*, and *Cylindrocystis brébissonii*, are the predominant taxa (Remias et al., 2012; Ling and Seppelt, 1990; Uetake et al., 2010; Takeuchi, 2013). In contrast, snow surfaces are mainly inhabited by green and red algae belonging to the order Chlamydomonadales, such as *Chlamydomonas* sp., *Chloromonas* sp., and *Sanguina nivaloides* (Davey et al., 2019; Segawa et al., 2018). Given their heterogeneity, it is essential to investigate the altitudinal and seasonal variability of their distribution and abundance to improve our understanding of their contributions to carbon cycling and glacier mass balance.

Urumqi Glacier No.1, located in the eastern Tien Shan Mountains, is frequently subject to dust storms that derive from surrounding deserts, resulting in substantial deposition of mineral particles on its ablation surface (Nagatsuka et al., 2014). These dust inputs foster the rapid formation and enlargement of cryoconite granules. A previous investigation has reported high areal coverage and biomass of cryoconite on ablation zone of this glacier, which is far exceeding observed on many Arctic glaciers (Takeuchi and Li, 2008). Within these granules, three morphologically distinct filamentous cyanobacterial taxa have been identified (Segawa et al., 2017); each potentially plays a different role in the initiation and structural development of granules (Chen et al., 2025). Moreover, micro-scale biogeochemical analyses have revealed active nitrogen cycling processes within cryoconite (Segawa et al. 2014, 2020; Murakami et al., 2022), suggesting the presence of nutrient hotspots that sustain microbial life on the oligotrophic supraglacial environment. However, previous studies have focused almost exclusively on the single time-point observations of cryoconite and ablation zone, with limited insight into the temporal dynamics of microbial communities across snow and ice surfaces during the melt season. Furthermore, although hydrological and meteorological observations on this glacier have

been conducted since the 1960s (Dong et al., 2012), continuous monitoring of microbial community dynamics has never been carried out, and the influence of biological processes on surface albedo has not been adequately considered. Therefore, conducting continuous observations during the biologically active melt season is essential for improving the accuracy of mass balance models and enhancing our understanding of bio-albedo feedbacks in glacier retreat.

This study has three main objectives: (1) to investigate the spatial and temporal distribution patterns of algal and cyanobacterial communities on glacial snow and ice surfaces of Urumqi Glacier No.1; (2) to identify key environmental drivers influencing variations in community structure; and (3) to evaluate the ecological role of phototrophic taxa (algae and cyanobacteria) and their potential impact on glacier surface albedo.

2 Study sites and methods

2.1 Study sites

Urumqi Glacier No.1, located at 43°06′N and 86°49′E, lies within the Tien Shan Mountains of the Xinjiang Uyghur Autonomous Region in western China (Fig. 1a). This northeast-facing glacier spans elevations from 3,752 to 4,445 m above sea level (a.s.l.). This glacier lost approximately 20% of its volume between 1962 and 2003, and it split into eastern and western branches in 1993 as a result of its continued retreat (Ye et al., 2005). The total catchment area is approximately 1.618 km^2 (Yue et al., 2022). Mass accumulation primarily occurs during the summer months, corresponding with peak precipitation rates. Hourly meteorological data, including air temperature, downwards solar radiation, precipitation, and snowmelt (in water equivalent), were obtained from ERA5-Land (0.1° × 0.1° resolution, 2 m above surface, https://cds.climate.copernicus.eu/datasets/reanalysis-era5-land?tab=download) for July 1 – August 31, 2013, and converted to daily means by averaging hourly values (Fig. 2). The mean annual equilibrium line altitude (ELA) in 2013 was 4,240 m a.s.l. (https://wgms.ch/products_ref_glaciers/urumqi/). This region is frequently influenced by dust storm activity due to the surrounding major deserts, with dust primarily originating from the Taklimakan Desert (Takeuchi et al., 2011; Li et al., 2010; Nagatsuka et al., 2014). The glacier's ablation zone is notably characterized by the widespread presence of cryoconite granules, with a mean dry weight of 335 g m^{-2} and an organic matter content of 9.4 ± 1.6%

(Takeuchi and Li, 2008). Cryoconite holes are generally absent from the glacier surface (Takeuchi and Li, 2008).

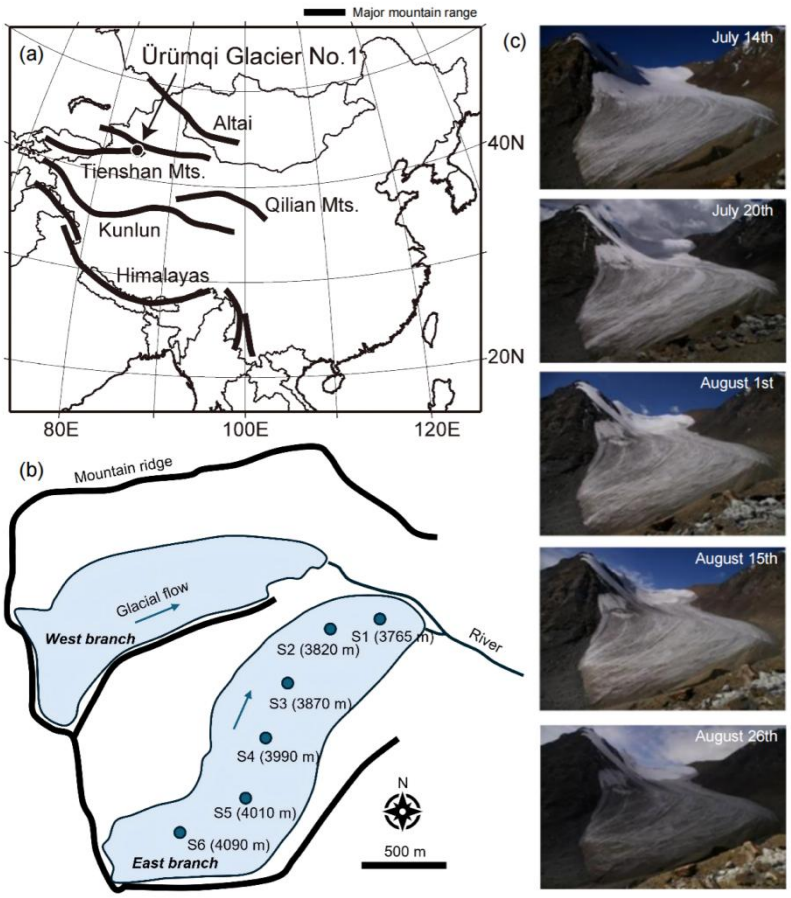

Figure 1: Location maps and photographs of Urumqi Glacier No.1. (a) Location of Urumqi Glacier No.1 in the Tien Shan Mountains. (b) Map of sampling sites (S1–S6) in this study. (c) Photographs of Urumqi Glacier No.1 across five sampling periods in 2013.

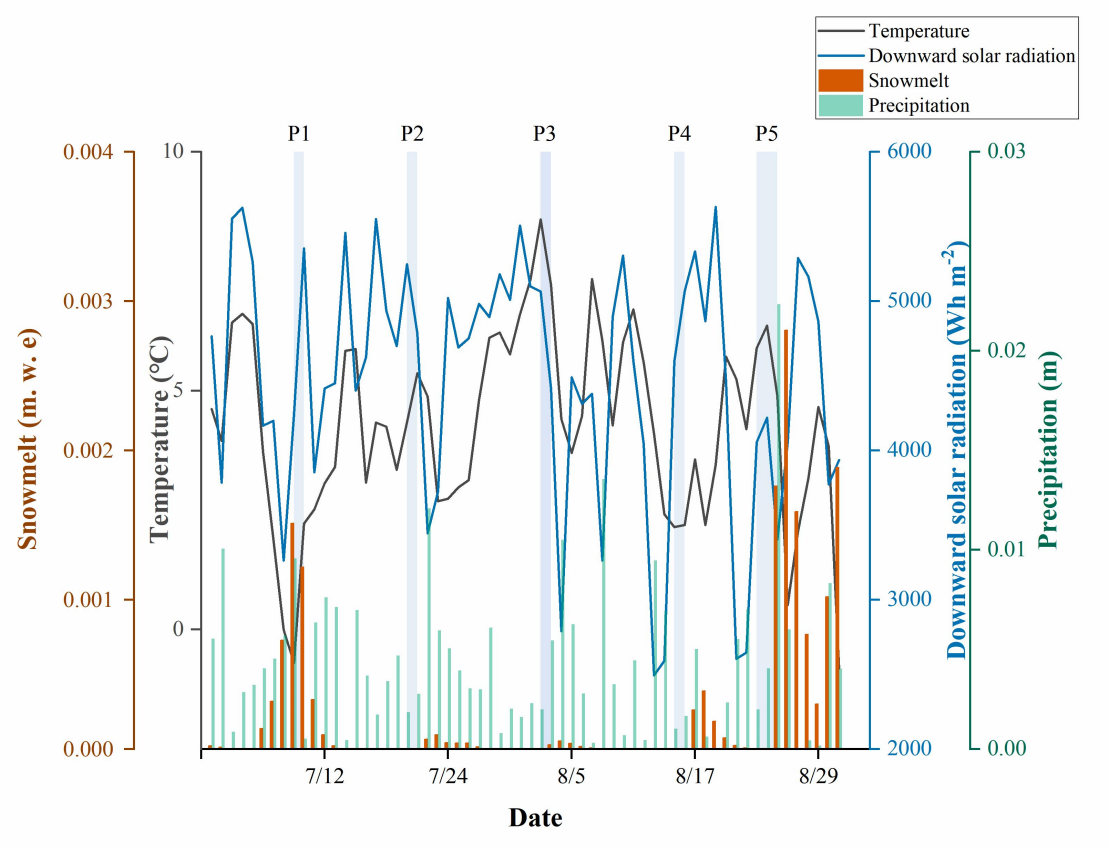

Figure 2: Meteorological datasets of Urumqi Glacier No.1 during July and August in 2013. P1-P5 denote sampling period.

2.2 Methods

2.2.1 Sampling collection

Field investigations were conducted five times in 2013, specifically on July 8–11 (P1), July 20–21 (P2), August 2–3 (P3), August 15–16 (P4), and August 24–26 (P5), across six sites on different altitudes (S1-S6, Fig. 1b, Fig. S1). During P1, S1–S4 were characterized by exposed ice surfaces, while S5 and S6 remained snow-covered (Fig. 1c). In the subsequent four sampling periods, ice surfaces extended upslope, resulting in S1 to S5 being classified as ice surfaces, with only S6 retaining a snow cover (Fig. 1c). Ice surface was characterized by widespread, dispersed cryoconite material, consistent with the patterns reported by Takeuchi and Li (2008). Surface ice and snow samples containing dispersed cryoconite were collected along the eastern branch of Urumqi Glacier No. 1 using a pre-cleaned stainless-steel scoop. Each sample covered an area of approximately 30–225 cm^2 and had a thickness of 1–2 cm (Table S1). For subsequent analysis, three to five samples were collected from randomly selected surface areas at each site. To preserve biological activity, samples were melted and fixed with

a 3% formalin solution in sterile 30 mL polyethylene bottles (IBOY, AS ONE, Japan). Additionally, one sample per site was collected and kept frozen without fixative for taxonomic identification of algal and cyanobacterial species. All samples were subsequently delivered to a laboratory at Chiba University for further analysis within six months of sampling.

2.2.2 Morphological identification of algae and cyanobacteria

Algal and cyanobacteria taxa were identified based on morphological observations using an optical microscope. To loosen sedimentary particles, each sample was ultrasonicated for 10 minutes. For each observed taxon, morphological characteristics and sizes, were recorded and compared with descriptions in previous studies (Takeuchi, 2004; Takeuchi et al., 2019; Segawa et al., 2017). Algae were identified using optical microscopy (BX51, Olympus, Japan). In contrast, cyanobacteria were highly difficult to distinguish from the abundant mineral particles and organic matter present in the samples under standard transmitted light; therefore, epifluorescence microscopy was employed for their detection. Cells were photographed at 400× magnification using randomly selected fields of view. Cell dimensions were measured from digital images using ImageJ software (National Institutes of Health, USA). For each taxon, approximately 60–100 cells were measured, and the mean values were used for subsequent analyses. Because filamentous cyanobacteria consisted of very small cells, images were captured at 1000× magnification to determine the average cell width and length. The biovolume of a single cell was calculated from the volumes of geometric analogs of cell morphology: cyanobacterial cells were modeled as cylinders, and algal cells were represented as ellipsoids or spheres.

2.2.3 Quantification of algal and cyanobacterial biovolume-based biomass

Cell abundance and biovolume-based biomass of algae and cyanobacteria at each sampling site was quantified by direct optical microscopic cell counting. Only cells showing chlorophyll autofluorescence were considered viable phototrophic microorganisms and included in the counts. A volume of 2–100 mL of meltwater was filtered through a polytetrafluoroethylene (PTFE) membrane filter (pore size 0.45 μm; JHWP01300, Merck Millipore, Germany), and cells retained on the filter were enumerated using an optical microscope (BX51, Olympus, Japan) by counting 1–3 randomly selected transects per filter. Each sample was counted in 3–5 times to ensure reproducibility. Unicellular taxa were counted as individual cells. For filamentous cyanobacteria, which cannot be counted as individual cells due to

their elongated trichomes, we quantified their abundance by counting them in standardized length units of 12.5 um using a calibrated microscope grid. This length unit corresponds to the average size of a single cell within the filament. These length counts were then converted to cell numbers based on the average cell dimensions determined for each taxon. Cell concentrations (cells mL^{-1}, Table S2) were calculated based on the average cell counts and the volume of water filtered. The total biovolume (mL) of snow and ice algae in each sample was calculated as the product of cell concentration (cells mL^{-1}) and the mean cell volume of each taxon (μm^3 $cell^{-1}$). Total biovolume-based biomass (μL m^{-2}) of algae and cyanobacteria was then estimated by biovolume (cell volume) per unit surface area The biovolume-based community composition (proportion) at each site was expressed as the relative abundance of each taxon to the total biovolume-based biomass. Mean values and standard deviations were calculated based on replicate samples collected from different surface areas at each site.

2.2.4 Major chemical solutes measurement

Major soluble ions in snow samples, including anions of NO_3^-, Cl^-, and SO_4^{2-} and cations of NH_4^+, K^+, Na^+, Mg^{2+}, and Ca^{2+}, were analyzed using an ion chromatography system (ICS-1100, Thermo Fisher Scientific, USA). Prior to analysis, melted samples were filtered through ion-free chromatographic discs (Chromate disk, pore size: 0.45 μm, GL Science, Japan) to eliminate particulate matter.

For anion analysis, a Dionex IonPac AS12A analytical column paired with an AG12A guard column was employed. The eluent consisted of a mixture of 2.7 mM Na_2CO_3 and 0.3 mM $NaHCO_3$, delivered at a flow rate of 1.5 mL min^{-1}. For cation analysis, a Dionex IonPac CS12A column was used with 20 mM methanesulfonic acid as the eluent, operating at a flow rate of 1.0 mL min^{-1}. The reported ionic composition represents only the major dissolved ions analyzed in this study and does not constitute a complete ionic charge balance, as dissolved species such as bicarbonate (HCO_3^-) were not included in the analytical protocol.

2.2.5 Determination of mineral and organic matter loads

The mass of organic and mineral matter per unit area of samples collected during P5 were determined using a loss-on-ignition (LOI) method. Samples were dried in pre-weighed crucibles at an electrical dryer (DO-450FA, As One, Japan) at 60°C for 24–48h until a constant mass was achieved. After cooling to room temperature, the samples were weighed to obtain the dry mass (m_d). The dried samples

were then combusted at 500°C for 3h in an electric furnace and reweighed after cooling to determine the combusted mass (m_c). Organic matter mass was calculated as the mass loss during combustion (m_d - m_c). The mineral fraction was estimated as the remaining mass after combustion. Five replicate samples were analyzed for each sampling site, and the mean value was calculated from the replicate measurements.

2.2.6 Statistical data analysis

Dissimilarities in community composition of algae and cyanobacteria, as well as in ion composition across sampling period and surface status (ice vs. snow), were assessed using permutational multivariate analysis of variance (PERMANOVA) based on Bray–Curtis distance matrices, implemented with the adonis function in the R package "vegan" (Oksanen et al., 2010). Spearman's rank correlation analysis was conducted in OriginPro to examine relationships between algal/cyanobacterial biovolume-based biomass and chemical variables. A two-way analysis of variance (two-way ANOVA) was used to evaluate the effects of surface status and sampling period on phototrophic biovolume-based biomass. Differences in major ion concentrations and mineral loads among sampling periods and surface conditions were evaluated using one-way analysis of variance (one-way ANOVA). All univariate statistical analyses were performed in OriginPro. Statistical significance was determined at $p < 0.05$.

3 Results

3.1 Observed algae and cyanobacteria on the glacier surface

Two taxa of algae and six taxa of cyanobacteria were identified on the glacier surface through microscopic observation (Table 1, Fig. 3). The morphological characteristic of each taxon was described as follows, in conjunction with findings from previous DNA-based studies (Segawa et al., 2017; 2023). Molecular analyses previously detected a total of 20 cyanobacterial operational taxonomic units (OTUs) on the glacier surface. These previous molecular frameworks were utilized as a reference to guide our morphological classification of the dominant active taxa.

Algae

(1) *Chloromonadinia* species

Cells were spherical in shape and lacked visible pyrenoids in the chloroplasts. Intracellular pigments

appeared green and red, and all observed cells were in the zygote stage. Mean cell diameter was 16.0 ± 1.8 μm.

(2) *Cylindrocystis brébissonii*

Cells were cylindrical with rounded apices, containing two chloroplasts each with a central pyrenoid. However, only one chloroplast was observed in short, divided cells. Cells measured 28.3 ± 6.0 μm in length and 17.6 ± 1.9 μm in width.

Cyanobacteria

(1) Oscillatoriaceae (Osc.) cyanobacterium 1

Trichomes lacked a sheath, and clear constrictions were visible between adjacent cells. Trichomes were 15–80 μm in length. Cells measured 2.0 ± 0.4 μm in length and 1.6 ± 0.2 μm in width..

(2) Oscillatoriaceae cyanobacterium 2

Trichome were enclosed within a colorless mucilaginous sheath. Green intracellular granules were observed within the cells. Trichomes were 20–430 μm in length. Cells measured 3.2 ± 0.8 μm in length and 3.1 ± 0.5 μm in width.

(3) Oscillatoriaceae cyanobacterium 3

Trichome were surrounded by a colorless mucilaginous sheath, without conspicuous internal structures. Trichomes were 20–260 μm in length. Cells measured 2.0 ± 0.3 μm in length and 1.5 ± 0.2 μm in width.

(4) Chroococcaceae (Chr.) cyanobacterium 1

Spherical cells were surrounded by with brown or yellow mucilaginous sheaths and occurred as solitary or paired cells forming small colonies. Mean cell diameter was 3.8 ± 0.6 μm.

(5) Chroococcaceae cyanobacterium 2

Spherical paired cells without apparent colonies. Mean cell diameter was 3.9 ± 0.6 μm.

(6) Chroococcaceae cyanobacterium 3

Spherical cells with a mean diameter of 2.7 ± 1.1 μm.

253 **Table 1 Morphological Characteristics of Identified Algae and Cyanobacteria**

Phototrophic taxa	Cell morphology	Size (μm, mean ± SD)	Metabarcoding data (reference)
Chloromonadinia species	Sphere	Diameter: 16.0 ± 1.8	*Chloromonadinia* species (Segawa et al., 2023)
Cylindrocystis brébissonii	Cylinder	Length: 28.3 ± 6.0; Width: 17.6 ± 1.9	No corresponding data
Oscillatoriaceae cyanobacterium 1	Filamentous cell	Trichomes: 15–80 Length : 2.0 ± 0.3 Width: 1.6 ± 0.2	*Pseudanabaena* (Segawa et al., 2017)
Oscillatoriaceae cyanobacterium 2	Filamentous cell	Trichomes: 20–430 Length : 3.2 ± 0.8 Width: 3.1 ± 0.5	*Microcoleus* (Segawa et al., 2017)
Oscillatoriaceae cyanobacterium 3	Filamentous cell	Trichomes: 20–260 Length : 2.0 ± 0.3 Width: 1.5 ± 0.2	Unclassified; *Oscillatoriales*; *Geitlerinema* (Segawa et al., 2017)
Chroococcaceae cyanobacterium 1	Sphere	Diameter: 3.8 ± 0.6	No corresponding data
Chroococcaceae cyanobacterium 2	Sphere	Diameter: 3.9 ± 0.6	No corresponding data
Chroococcaceae cyanobacterium 3	Sphere	Diameter: 2.7 ± 1.1	No corresponding data

254

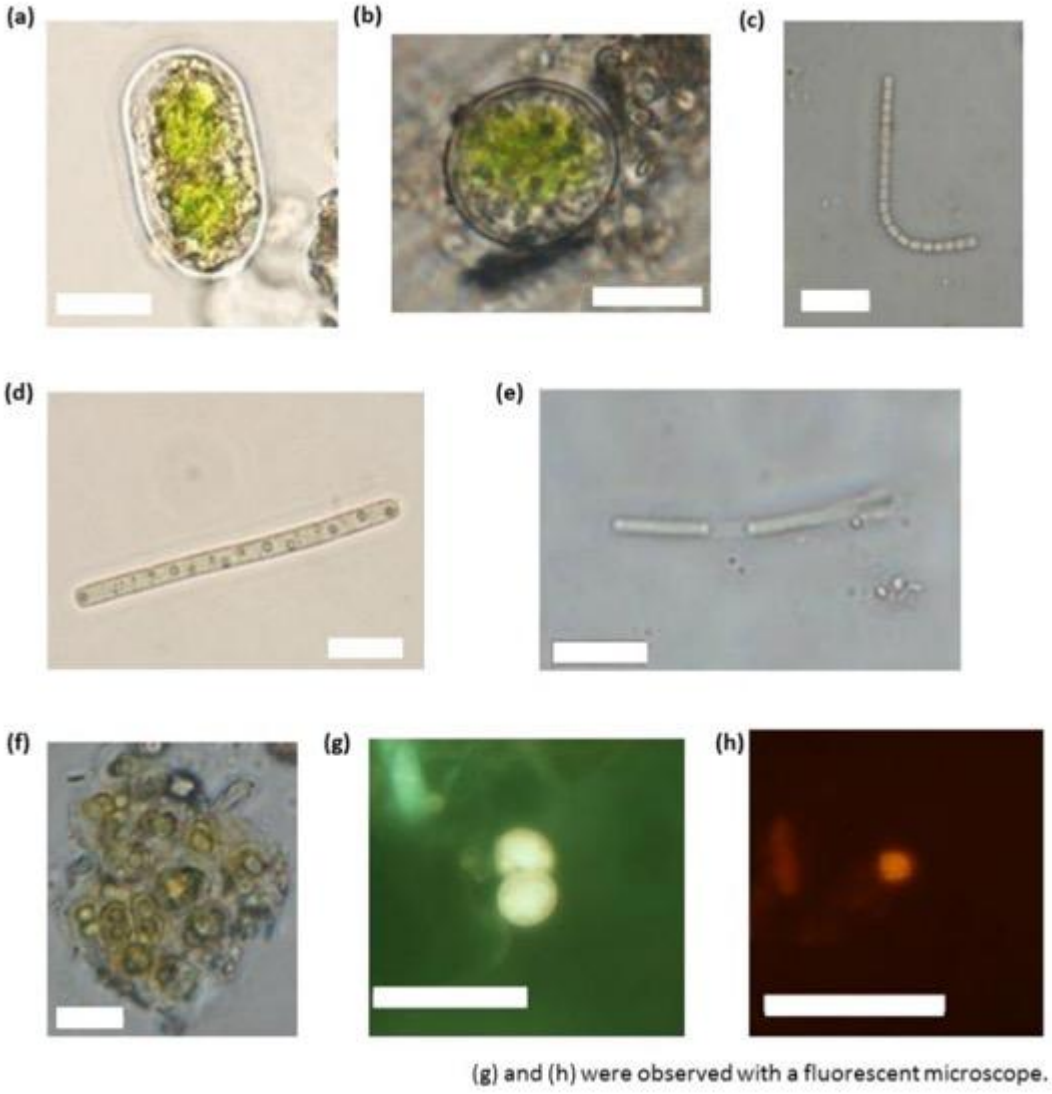

255

256 **Figure 3: Photographs of algae and cyanobacteria observed on surface of Urumqi Glacier No.1. (a)**
257 ***Cylindrocystis brébissonii*; (b) *Chloromonadinia* species; (c) Oscillatoriaceae cyanobacterium 1; (d)**
258 **Oscillatoriaceae cyanobacterium 2; (e) Oscillatoriaceae cyanobacterium 3; (f) Chroococcaceae**
259 **cyanobacterium 1; (g) Chroococcaceae cyanobacterium 2; (h) Chroococcaceae cyanobacterium 3. Scale bar**
260 **= 10 μm**

261 **3.2 Seasonal and spatial variations in the total biomass of algae and cyanobacteria**

262 The total biovolume-based biomass of algae and cyanobacteria on the glacier surface remained
263 relatively stable through the melt season (two-way ANOVA, $p = 0.62 > 0.05$, Fig. 4). However, a
264 marked increase in total biomass was observed when the snow surface transitioned to bare ice at the
265 midstream sites (S4 and S5). At S4, biomass increased markedly from P1 to P2 (from 4.7 to 419.1 μL
266 m^{-2}). At S5, although the biomass in P1 (3.7 μL m^{-2}) was not significantly different from that in P2 (1.2
267 μm^{-2}), a significant increase was observed in P3, with biomass reaching 278.3 μL m^{-2}. During P5,

biomass on ice surface (S1-S5) remained at comparable levels. Overall, the total biovolume-based biomass on the ice surface was significantly higher than that on the snow surface (two-way ANOVA, $p = 0.03 < 0.05$).

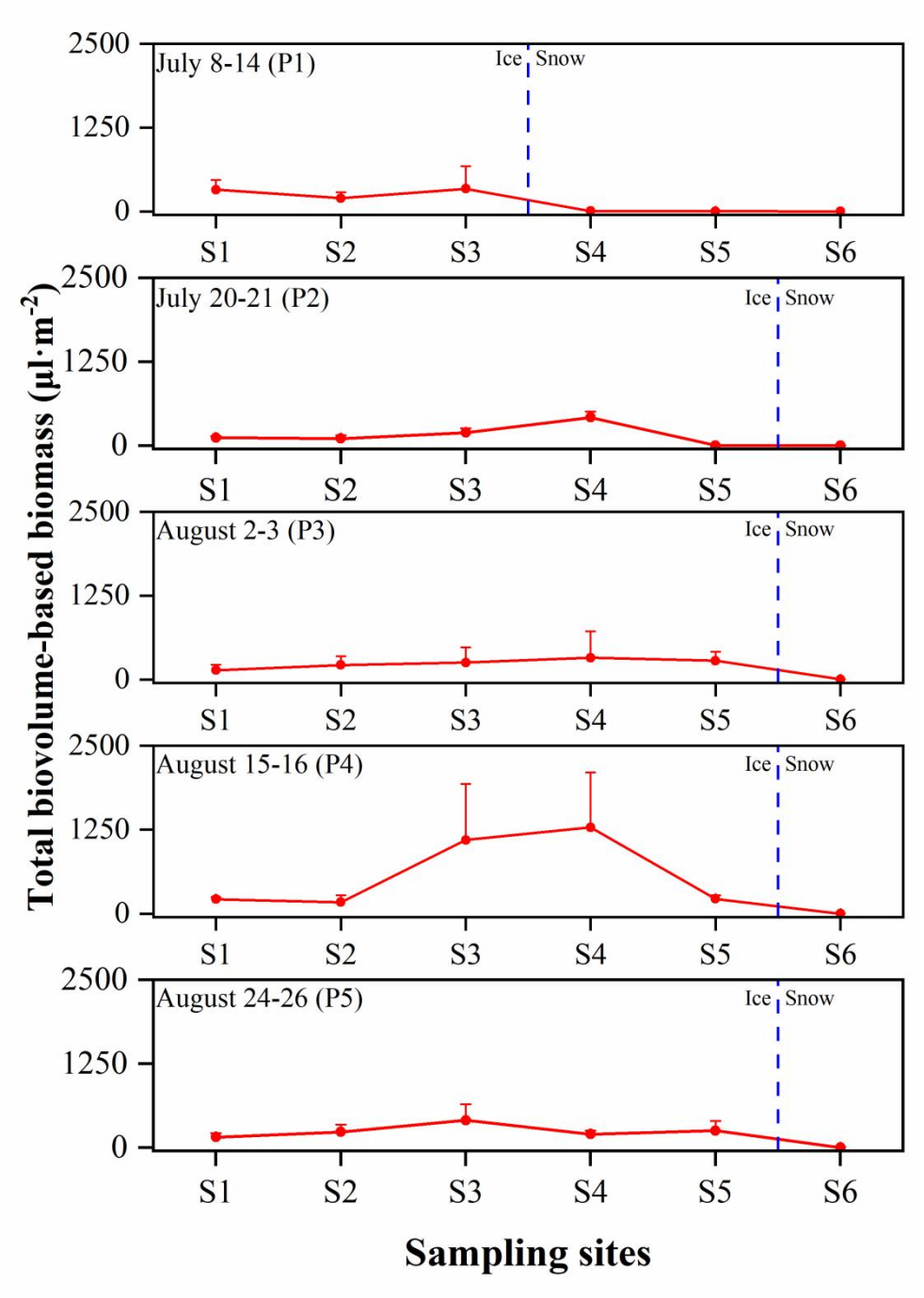

Figure 4: Seasonal and spatial variations in the total biovolume-based biomass of algae and cyanobacteria on Urumqi Glacier No.1 from July to August 2013. The blue dashed line represents the boundary between the snow and ice surface.

3.3 Spatiotemporal changes of algal and cyanobacterial community composition on glacier surfaces

The relative dominance of algae and cyanobacteria varied primarily with surface status rather than sampling period (Fig. 5). PERMANOVA analysis detected no significant differences in community composition among sampling periods ($p > 0.05$), whereas significant differences were observed between snow-covered and ice surfaces ($p < 0.01$). Across all sampling periods, snow surfaces were consistently dominated by algal taxa, primarily *Chloromonadinia* species, whereas cyanobacteria predominated on bare ice surfaces.

A clear upstream shift in cyanobacterial dominance accompanied the seasonal expansion of bare ice. During P1, filamentous cyanobacteria were dominant on downstream ice-covered sites (S1–S3), accounting for 61–75% of the total biovolume-based biomass, whereas the snow-covered upstream sites (S4–S6) were prevailed by *Chloromonadinia* species, contributing 65–92% in biovolume-based community composition. By P2, cyanobacterial dominance had expanded upstream and Chloromonadinia species remained dominant only at S5 and S6. From P3 onward, filamentous cyanobacteria consistently dominated sites S1–S5, while *Chloromonadinia* species remained dominant solely at the uppermost site (S6). The only exception occurred during P4, when filamentous cyanobacteria dominated all sites, accounting for 61–84% of the total biomass.

Among the algal taxa, *Chloromonadinia* species were the principal constituents of snow communities throughout the study, accounting for 16–92% of the total biomass. In contrast, *Cylindrocystis brébissonii* was detected exclusively on ice surfaces and occurred sporadically at one or two sites during each sampling period, representing less than 1.5% of the total biomass.

Filamentous Oscillatoriaceae cyanobacteria constituted the dominant component of ice-surface communities during sampling period. Osc. cyanobacterium 1 showed a clear preference for ice surfaces, with biomass generally rising from P1 to P4, particularly at mid- to up-glacier ice sites. In contrast, its biomass on snow surfaces remained negligible throughout the sampling period, rarely exceeding 0.1 μL m^{-2} (Fig. S2).

Osc. cyanobacteria 2 and 3 were the most abundant cyanobacterial taxa, constituting 65%–95% of the total cyanobacterial biovolume-based biomass across all ice sites and sampling periods. Their biomass increased progressively from P1 to P4, with the highest values recorded at sites S3 and S4 during P4, where Osc. cyanobacterium 2 exceeded 300 μL m^{-2} and Osc. cyanobacterium 3 surpassed

470 μL m^{-2}. From P4 onward, a distinct spatial pattern emerged: Osc. cyanobacterium 2 dominated the downstream sites (S1–S2), whereas Osc. cyanobacterium 3 became dominant at the upstream sites (S3–S5). In contrast, both taxa showed very low biovolume-based biomass on snow-covered surfaces, with biomass consistently below 1 μL m^{-2}.

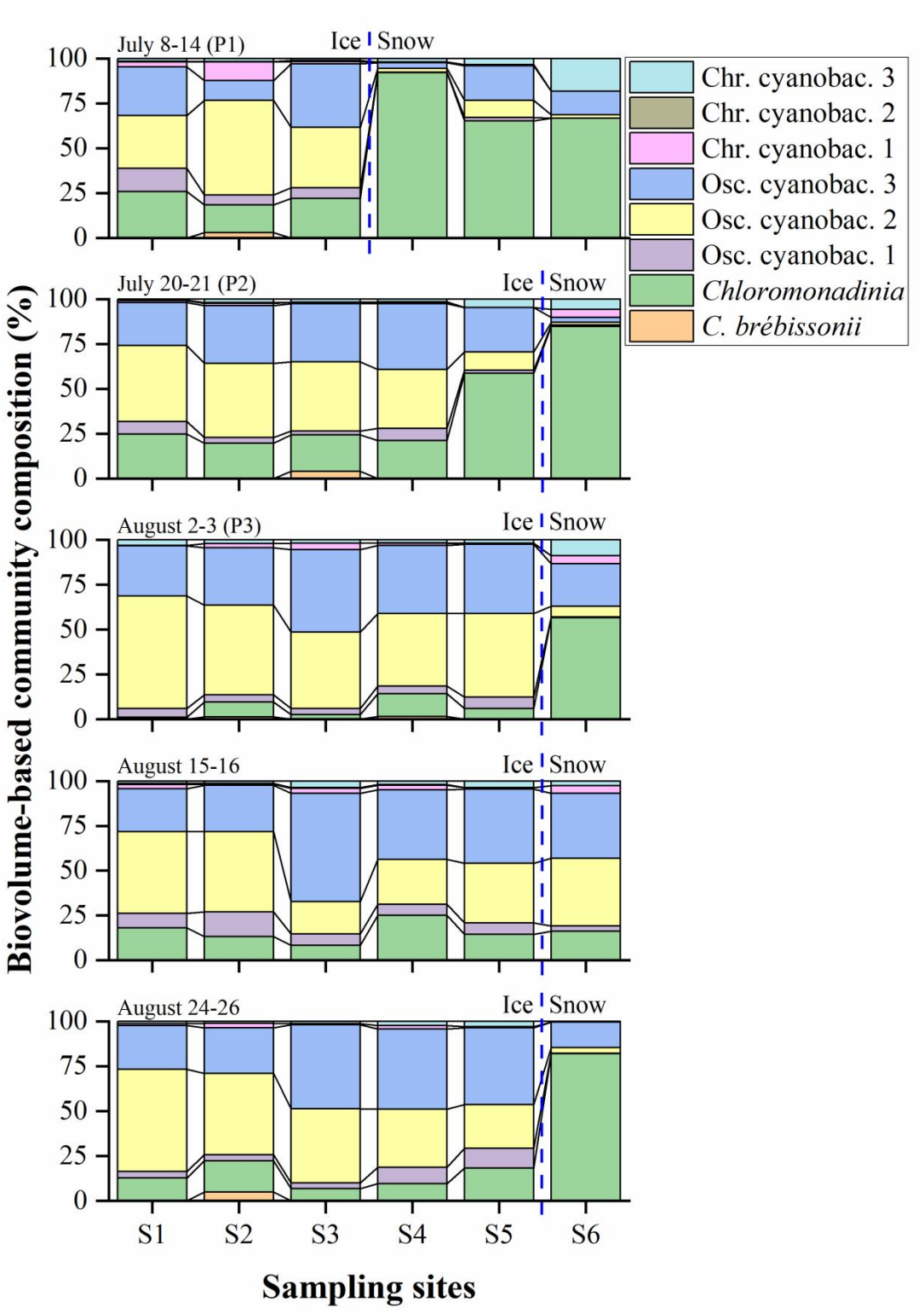

Figure 5: Seasonal variations in the biovolume-based community composition of algae and cyanobacteria at sampling sites (S1–S6) across five sampling periods (P1–P5). The dashed line represents the boundary between the snow and ice surface.

Among the unicellular cyanobacteria, Chr. cyanobacterium 1 showed a noticeable biomass increase

by P4 on ice, reaching up to ~30 μL m^{-2} at S3 and S4. Chr. cyanobacteria 2 and 3 maintained relatively low abundance levels throughout all sampling sites and periods, with slight elevations observed on ice during P4. All three Chroococcaceae taxa were almost absent on snow surfaces (biomass < 0.13 μL m^{-2}) .

3.4 Variations in chemical conditions across the sampling period and surface status

The concentrations of major ions showed notable temporal variation throughout the five sampling periods (Fig. 6). SO_4^{2-}, NO_3^-, K^+ and Mg^{2+} concentrations temporally varied significantly among sampling periods (one-way ANOVA, $p < 0.01$). SO_4^{2-} and NO_3^- both peaked in P1 (= 12.9 and = 6.8 μEq L^{-1}, respectively), declined sharply in P2, and showed secondary increases in P5. In contrast, K^+ remained stable in early periods (~5 μEq L^{-1}) before declining to its lowest level in P5 (= 1.7 μEq L^{-1}). Mg^{2+} exhibited elevated concentrations in P1 and P3 (= 20.3 and = 25.9 μEq L^{-1}), dropped markedly to 8.6 μEq L^{-1}in P4, and partially rebounded to 11.3 μEq L^{-1} in P5.

Significant differences in ion concentrations were also observed between surface status (ice vs. snow) (one-way ANOVA, $p < 0.01$, Fig. 6b). Ice surfaces consistently hold higher mean concentrations of crustally derived ions, including Ca^{2+} (125.5 vs. 22.6 μEq L^{-1}), Mg^{2+} (20.6 vs. 5.9 μEq L^{-1}), Na^+ (12.5 vs. 5.3 μEq L^{-1}) and K^+ (4.9 vs. 1.3 μEq L^{-1}). In contrast, snow surfaces showed higher concentrations of NO_3^- (2.3 vs. 6.0 μEq L^{-1}), SO_4^{2-} (6.3 vs. 10.1 μEq L^{-1}), and NH_4^+ (2.6 vs. 8.0 μEq L^{-1}).

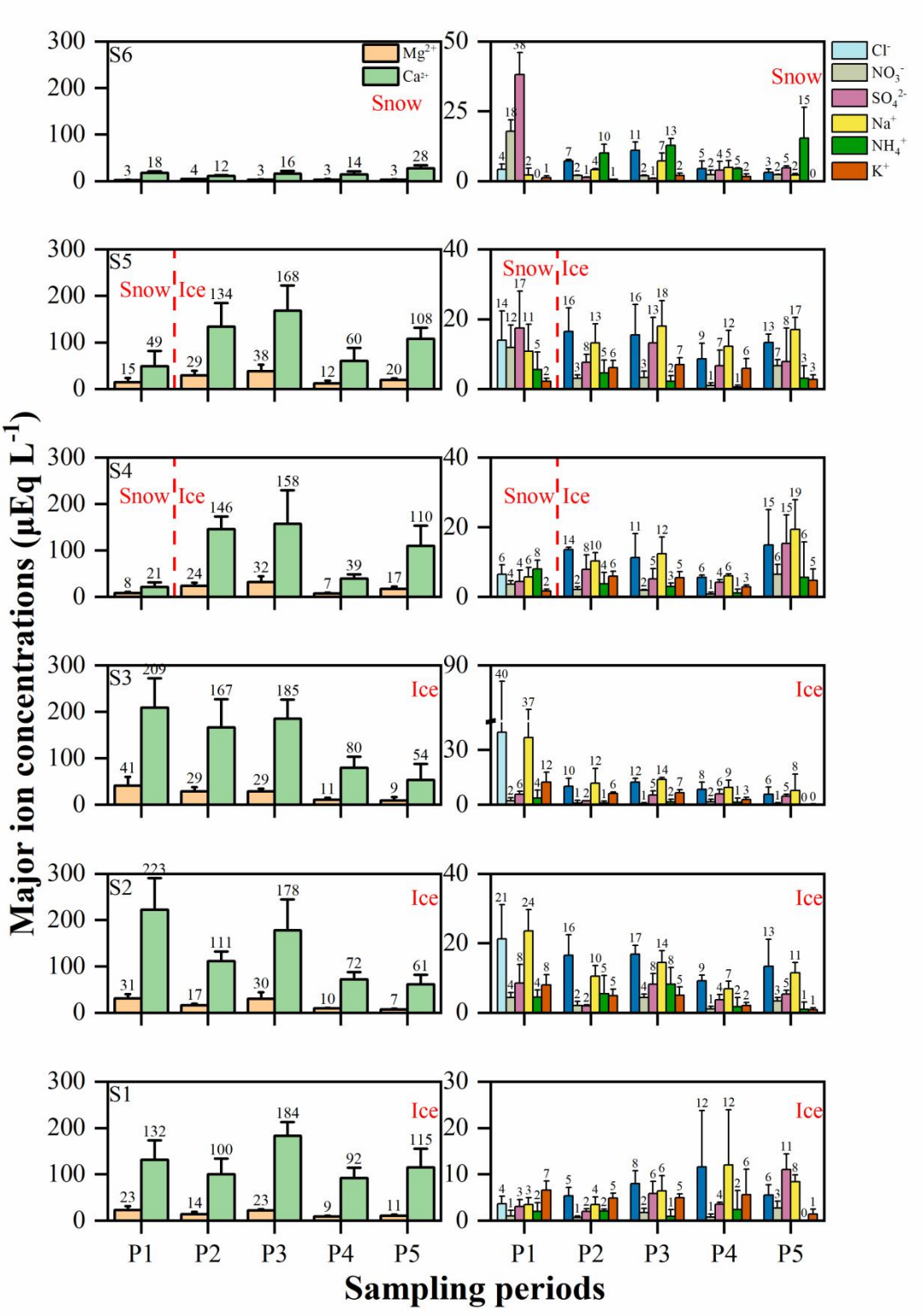

Figure 6: Spatial and temporal variations in major ion concentrations at six sampling sites (S1–S6) across five sampling periods (P1–P5). Red dashed line represents the boundary between the snow and ice surface.

3.5 Mineral and organic matter loads on glacier surface

Mineral matter constituted the dominant fraction (> 88.2%) in samples collected on ice surface

(S1–S5) during P5, accounting for 185.7–314.6 g m^{-2}, whereas organic matter represented a much smaller proportion, ranging from 15.5 to 42.0 g m^{-2} (Table S4). No significant differences in mineral fractions were observed among sampling sites (one-way ANOVA, $p > 0.05$), whereas organic fractions varied significantly among sites (one-way ANOVA, $p < 0.05$).

4 Discussion

4.1 Algal community dynamics in response to glacier surface transition

The biomass of snow/glacier algae on Urumqi Glacier No.1 remained consistently low with minimal temporal variation, suggesting that algal proliferation is highly constrained in this environment. Previous studies have shown that glacier algal blooms on the Greenland Ice Sheet are strongly promoted by the availability of mineral phosphorus released from aeolian dust (McCutcheon et al., 2021). Despite the abundance of mineral particles on the Urumqi Glacier No. 1, glacier algae kept a low biomass on the surface, suggesting that factors other than dust abundance, such as phosphorus bioavailability or local environmental conditions, may limit glacier algal establishment in this region. *Chloromonadinia* species was found on both snow and ice but showed a clear preference for snow, aligning with its classification as a snow-environment specialist (Takeuchi, 2001), similar to observations in the Himalayas (Yoshimura et al., 1997) and Altai Mountains (Takeuchi et al., 2006). All observed Chloromonadinia cells were in the zygote stage, characterized by orange-red pigmentation. All observed *Chloromonadinia* cells were in the zygote stage, characterized by orange-red pigmentation. The exclusive occurrence of zygotes indicates that this taxon was present predominantly in a dormant or resistant life stage rather than as an actively growing population.

Conversely, the green alga *C. brébissonii* was restricted to ice surfaces. Despite its presence, its sporadic and low abundance suggest it functions as an ice-specialist that fails to establish stable, large-scale populations on this glacier, contrasting with earlier classifications that often regard certain *Cylindrocystis* strains as opportunists with broader habitat ranges (Kol, 1942; Remias et al., 2012).

On this glacier, the role of algae in surface darkening is habitat-dependent. On snow, despite low biomass, *Chloromonadinia* species is likely the primary biological agent for albedo reduction due to the absence of cryoconite. However, on bare ice, the direct contribution of eukaryotic algae to surface darkening may be secondary to that of cyanobacteria and mineral particles, primarily due to the

overwhelming biomass dominance of filamentous cyanobacteria and the heavy loading of lithogenic dust observed throughout the melt season. This is consistent with studies suggesting that while snow algae can significantly lower albedo in the early melt season, their impact is often overshadowed by other light-absorbing particles (e.g., cryoconite) once the ice is exposed (Lutz et al., 2016; Di Mauro et al., 2020).

4.2 Phylogenetic lines of the cyanobacterial microscopic morphotypes

Previous DNA metabarcoding studies on Urumqi Glacier No. 1 detected approximately 8 cyanobacterial operational taxonomic units (OTUs) (Segawa et al., 2017), whereas microscopic observation in this study identified six cyanobacterial morphotypes and two algal taxa. This numerical difference reflects the complementary nature of the two approaches rather than an inconsistency between the datasets. DNA metabarcoding is highly sensitive and captures the full taxonomic inventory of glacier microorganisms, including rare, dormant, or transient taxa introduced by atmospheric deposition. In contrast, microscopic observation coupled with chlorophyll autofluorescence selectively captures structurally intact, pigment-bearing phototrophs, enabling the direct quantification of cell abundance and biomass.

Consistent with previous molecular data, our dominant filamentous morphotypes corresponded with major filamentous cyanobacterial OTUs previously reported from these sites, such as *Microcoleus*, *Pseudanabaena*, and *Geitlerinema* (Table 1; Segawa et al., 2017). Despite the greater OTU richness revealed by high-throughput sequencing, the bulk of the phototrophic biomass during the melt season was contributed by only two dominant Oscillatoriaceae morphotypes, which drove the clear spatial and seasonal succession observed across the glacier. These findings demonstrate that while DNA metabarcoding provides a comprehensive taxonomic inventory, microscopic quantification is indispensable for identifying the specific dominant taxa responsible for actual biomass accumulation and community dynamics. Taken together, integrating molecular checklists with morphological biomass estimation yields a more holistic understanding of supraglacial phototrophic communities.

4.3 Cyanobacterial dominance and its role in surface darkening

In contrast to the ephemeral nature of snow algae, the cyanobacterial community on Urumqi Glacier No. 1 exhibited remarkable temporal stability in total biovolume-based biomass, albeit with significant

spatial and taxonomic shifts. While unicellular Chroococcaceae maintained low biomass, filamentous cyanobacteria (Oscillatoriaceae) sustained dominance on ice surfaces throughout the melt season. This persistent presence suggests their potential role in surface darkening through two primary pathways: direct organic pigmentation and the structural aggregation of mineral particles into stable, dark cryoconite granules (Takeuchi, 2009; 2013).

The spatial distribution of these dominant filamentous cyanobacteria revealed a distinct altitudinal zonation from P4 onwards, despite uniform geochemical characteristics across the glacier. Osc. cyanobacterium 2 dominated the downstream sites (S1–S2), whereas Osc. cyanobacterium 3 prevailed at the mid-to-up-glacier sites (S3–S5). This niche partitioning is likely driven by physical factors associated with altitude, specifically the duration of bare-ice exposure. The downstream sites (S1–S2) experience the earliest snow disappearance and the longest continuous melt season, allowing for the prolonged accumulation and structural stabilization of ice-surface microbial communities (Hodson et al., 2010; Uetake et al., 2016). The dominance of Osc. cyanobacterium 2 at these lower-elevation sites suggests an association with more developed, stable cryoconite habitats characterized by cumulative dust aggregation. In contrast, the mid-to-up glacier sites (S3–S5) encounter a much shorter exposure window. The dominance of Osc. cyanobacterium 3 in these upper areas, including a sharp increase in detectable biomass (exceeding 470 μL m^{-2}) during P4, indicates that this taxon is a potential pioneer microorganism well-adapted to recently exposed ice surfaces (Ortiz-Álvarez et al., 2018; Bradley et al., 2023). This apparent biomass spike was likely driven by the removal of the seasonal snow cover, which newly uncovered the underlying resident cyanobacterial cells on the ice surface. Alternatively, its prevalence at higher elevations may reflect a greater physiological tolerance to recurrent freeze–thaw cycles.

This altitudinal segregation implies that the cyanobacterial community is a strategically partitioned system rather than a monolithic assemblage. For instance, different cyanobacterial taxa may contribute uniquely to cryoconite granule formation (Chen et al., 2025) and vary in their capacities for light utilization and nutrient cycling (Murakami et al., 2022). The presence of multiple dominant taxa with distinct spatio-temporal peaks ensures that the glacier surface maintains high biological biomass across a wide range of environmental conditions—from stable lower reaches to dynamic, highly disturbed upper reaches. Consequently, the functional diversity within the Oscillatoriaceae contributes to the persistence and expansive spatial extent of biological darkening across the entire ablation zone.

Unlike the ephemeral algal blooms on Arctic glaciers (Takeuchi, 2013), the biological impact on Urumqi Glacier No. 1 is stabilized by the formation and multi-year persistence of cryoconite granules driven by filamentous cyanobacteria. While polar glacier algae, such as *Anancylonema nordenskiöldii*, exhibit explosive seasonal growth dynamics (Stibal et al., 2017; Onuma et al., 2023), the cyanobacterial biomass on Urumqi Glacier No. 1 remained relatively constant throughout the melt season. This lack of a seasonal spike suggests a fundamentally distinct ecological strategy: while polar ice algae thrive through opportunistic, rapid seasonal blooms, the cyanobacteria here rely on the long-term retention of stable structural aggregates. These filamentous taxa produce extracellular polymeric substances (EPS) that trap mineral dust, forming dark, spherical granules (Musilova et al., 2016; Segawa et al., 2017) that can persist and grow over multiple melt seasons (Takeuchi et al., 2010). This prolonged development facilitates the accumulation of refractory humic substances, significantly enhancing the cumulative light-absorbing capacity of the aggregates (Takeuchi, 2002).

Crucially, the spatial manifestation of these aggregates differs fundamentally from polar systems. On polar ice sheets, cryoconite is often concentrated within localized cryoconite holes, rendering its sheet-wide albedo impact secondary to vast, distributed ice algal blooms (Cook et al., 2020). Conversely, the bare-ice surface of Urumqi Glacier No. 1 is extensively covered by dispersed cryoconite rather than discrete holes (Takeuchi and Li, 2008). The high spatial occupancy of this dispersed material, combined with its structural stability provided by the cyanobacterial matrix, helps retain these dark, humic-rich aggregates on the ice surface even during minor scouring events. While literature suggests that consolidated organic-inorganic aggregates exert localized radiative impacts (Cook et al., 2016; Hotaling et al., 2021), the proliferation and retention of these filamentous taxa represents a key biological factor, interacting alongside heavy mineral dust loading, that drives the persistent and cumulative surface darkening observed on this Central Asian glacier.

4.4 Environmental drivers: Nitrogen limitation and mineral-derived ions

The distinct community compositions on snow and ice surfaces suggest different environmental controls. We found significant negative correlations between inorganic nitrogen concentrations (NO_3^- and NH_4^+) and the relative abundance of dominant filamentous cyanobacteria (Oscillatoriaceae) ($p < 0.05$; Fig. 7). This statistical trend indicates a close coupling between inorganic nitrogen availability

and cyanobacterial proliferation on the ice surface. Rather than implying a one-way causal advantage, this negative correlation may reflect the progressive biological drawdown of available nutrients by the high-biomass cyanobacterial mats during their active growth phase, a process supported by their metabolic pathways for efficient nutrient utilization and recycling within the cryoconite micro-habitats (Segawa et al., 2014; 2020; Murakami et al., 2022).

Furthermore, although no significant relationship was observed between Oscillatoriaceae biomass and the mineral fractions during P5, potentially due to the limited sample size, Oscillatoriaceae biomass was positively correlated with mineral-derived ions (Ca^{2+}, Mg^{2+}, and K^{+}, $p < 0.05$, Fig. 7). In Central Asian glacier systems, intense atmospheric dust deposition and subsequent lithogenic mineral weathering strongly govern the meltwater chemistry, making these dissolved cations reliable indicators of mineral influence (Li et al., 2006; Wu et al., 2012). The concentrations of these ions on Urumqi Glacier No.1 are substantially higher than those reported for Arctic glaciers, such as those in Svalbard, where mineral-derived ion concentrations are significantly lower due to limited dust input (Takeuchi et al., 2019). While glacier algae (such as *Ancylonema* spp., formerly *Ancylonema*) are commonly reported to dominate the low-mineral environments of Svalbard glaciers (Stibal et al., 2017), the high mineral availability on Urumqi Glacier No.1 provides a more suitable substrate and nutrient base for the proliferation of filamentous cyanobacteria and the subsequent development of cryoconite granules. This stark contrast in geochemical conditions explains why the primary biological drivers of albedo reduction differ so fundamentally between Central Asian and Arctic glacial systems—where the former relies on dust-mediated cyanobacterial aggregation (Segawa et al., 2010; Takeuchi and Li, 2008) and the latter is driven by widespread blooms of specialized eukaryotic ice algae (Williamson et al., 2018; Cook et al., 2020).

This relationship highlights the critical importance of mineral availability for cyanobacterial colonization and granule formation. Our results mirror observations from the Greenland Ice Sheet, where phosphorus and mineral availability are key drivers of cyanobacterial growth (Uetake et al., 2019), but this effect is likely amplified on Urumqi Glacier No.1 due to the extreme dust deposition characteristic of Central Asian mountains. In contrast, algal taxa showed no such correlations, suggesting their distribution may be driven by stochastic colonization or micro-scale physical factors like meltwater flow rather than macro-scale chemical parameters (Stibal et al., 2012a).

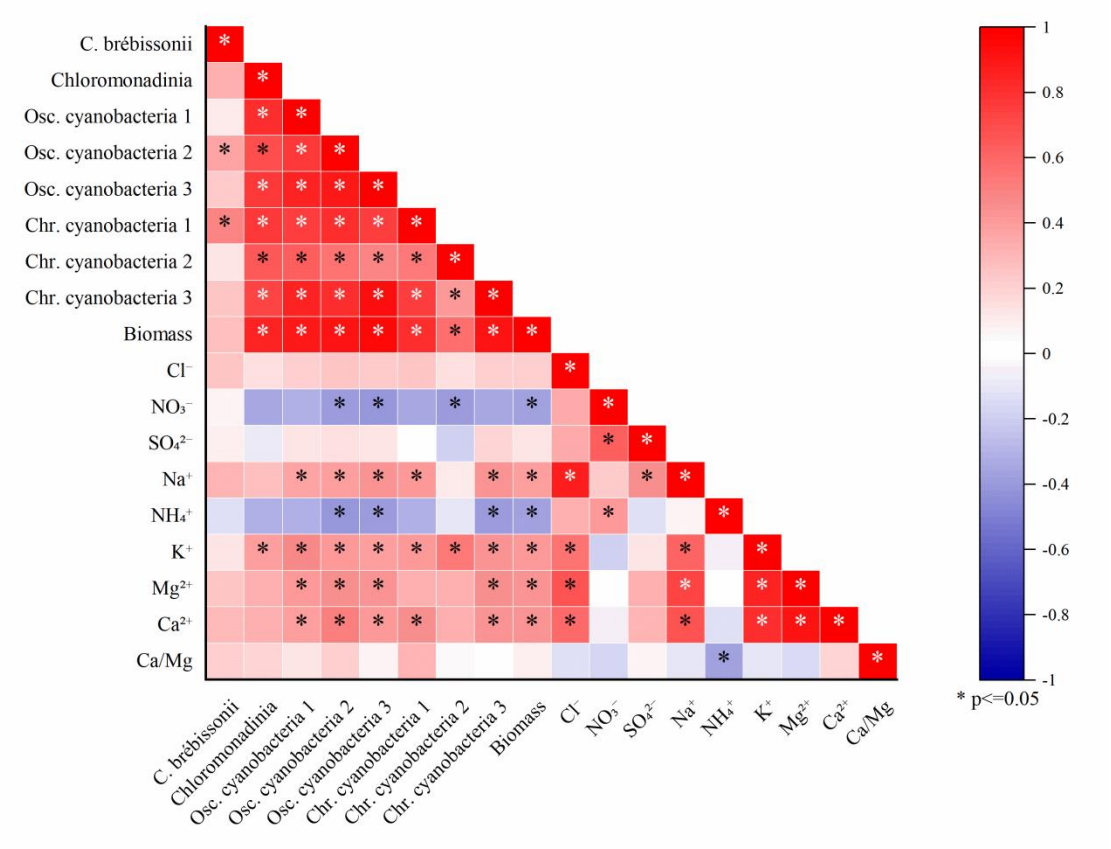

Figure 7: Correlation between major ion concentration and bio-volume of each algal and cyanobacterial taxa.

4.5 Ecological Implications and comparison with Arctic glaciers

One of the most significant ecological findings of this study is the complete absence of glacier algae, such as *Ancylonema* spp., which are the primary drivers of ice darkening on Arctic glaciers (e.g., Alaska, Svalbard) (Takeuchi 2013; Takeuchi et al., 2019). In polar regions, these Zygnematalean algae bloom on the ice surface, producing dark purple pigments that significantly reduce albedo (Williamson et al., 2018; Remias et al., 2012). However, on Urumqi Glacier No.1, this niche is predominantly occupied by a stable, cyanobacteria-dominated community.

The absence of *Ancylonema* and the corresponding dominance of filamentous cyanobacteria (Oscillatoriaceae) are likely attributable to the unique geochemical and physical environment of Central Asia. Takeuchi et al. (2019) demonstrated that Arctic glaciers in Svalbard are characterized by extremely low mineral ion concentrations, a condition that appears to favor the proliferation of free-living glacier algae. In contrast, the high dust flux on Urumqi Glacier No.1 provides an abundance of mineral cations, resulting in substantially elevated ionic concentrations. For example, mean Mg^{2+}

and Ca^{2+} concentrations on Urumqi Glacier No. 1 are approximately 13 and 59 times higher, respectively, than those reported for Svalbard (Mg^{2+}: 20.6 vs. 1.6 μEq L^{-1}; Ca^{2+}: 125.5 vs. 2.1 μEq L^{-1}, Takeuchi et al., 2019). These elevated mineral inputs maintain a higher pH on the ice surface. The high influx of carbonate-rich mineral dust from surrounding arid regions acts as a powerful geochemical buffer, maintaining the meltwater pH in a neutral-to-alkaline range (typically 7.5–8.5; Li et al., 2007; Wu et al., 2012). Such alkaline, mineral-rich conditions may be physiologically inhibitory to Anancylonema (formerly Ancylonema), which typically thrives in the more acidic, ultra-oligotrophic environments characteristic of polar ice (Remias et al., 2012; McCutcheon et al., 2021).

Furthermore, the physical presence of massive mineral dust promotes the formation of cryoconite granules. As revealed by Segawa and Takeuchi (2010) on Qiyi Glacier and further elucidated by Chen et al. (2025) on Urumqi Glacier No.1, filamentous cyanobacteria act as "ecosystem engineers," trapping mineral particles to form stable, spherical aggregates. This process may physically exclude glacier algae by reducing the availability of "clean" ice surfaces required for their colonization.

These results suggest that biological darkening on Central Asian glaciers may differ from the algal bloom, dominated patterns commonly reported for Arctic glaciers. While Arctic darkening is often ephemeral and sensitive to seasonal snowmelt timing, the darkening on Urumqi Glacier No.1 is more persistent due to the structural stability of cyanobacterial cryoconite. Therefore, applying Arctic-based bio-albedo models to Central Asian glaciers may lead to significant errors, highlighting the need for region-specific models that account for high mineral loading and its role in shaping microbial community structures.

5 Conclusion

This study characterized the spatio-temporal dynamics of phototrophic communities on Urumqi Glacier No. 1, revealing an ecological structure fundamentally distinct from those of better-studied polar glacial systems. The primary finding of this research is the clear biological succession driven by the seasonal transition of the glacier surface. As the snowpack recedes, the community shifts from the dominance of snow algae (*Chloromonadinia* species) to a massive proliferation of filamentous cyanobacteria (Oscillatoriaceae) on the exposed bare ice. This transition is marked by a significant increase in total biomass and the establishment of a stable microbial community that persists throughout the melt season.

Crucially, this study highlights the absence of eukaryotic glacier algae such as *Anancylonema* spp., which are the primary drivers of ice darkening on Arctic glaciers. Instead, the biological darkening process on Urumqi Glacier No. 1 is governed by the extensive development of these filamentous cyanobacterial mats interacting with abundant mineral particles. Our results demonstrate that the proliferation of dominant filamentous cyanobacteria is closely linked to high concentrations of mineral-derived ions and low inorganic nitrogen levels. This geochemical environment, shaped by high dust input from surrounding arid regions, appears to provide a specialized niche that favors cyanobacterial colonization and the structural development of cryoconite granules over the growth of eukaryotic glacier algae. Furthermore, we identified an altitudinal niche partitioning within the Oscillatoriaceae, where different taxa (e.g., Osc. cyanobacterium 2 and 3) dominate based on the altitudinal gradient and the corresponding duration of bare-ice exposure. This functional diversity ensures that a high biological biomass is maintained across the entire ablation zone.

The ecological implications of these findings are essential for predicting the future of alpine glaciers in a changing climate. Unlike the ephemeral algal blooms observed in Arctic regions, the darkening on Urumqi Glacier No. 1 is driven by structurally stable cryoconite granules that potentially persist across melt seasons. This prolonged development facilitates the accumulation of refractory humic substances, creating a more constant and resilient bio-albedo feedback pathway. Under projected warming scenarios, including extended melt seasons and increased dust deposition, the expansion of these cyanobacterial communities may further accelerate glacier mass loss. Therefore, it is imperative to integrate region-specific microbial dynamics, characterized by the absence of glacier algae and the dominance of mineral-buffered, long-lived cyanobacterial aggregates, into global glacier melt models to improve the accuracy of water resource projections in Central Asia.

Data availability

The datasets generated and analyzed during the current study are available from the corresponding author upon reasonable request. The datasets are currently not deposited in a public repository due to institutional data management policies of the affiliated university. The corresponding author is willing to provide access to the data for research purposes upon reasonable request and following confirmation

555 of compliance with institutional requirements.

556 **Author contributions**

557 YC and NT designed the study. YC and NT wrote and revised the manuscript with supports of XH and
558 WZ. ST collected samples and quantified biomass of algae and cyanobacteria. NT measured ion
559 concentration. YC and SL statistically analyzed data and draw figures. ZL organized the field
560 investigation.

561 **Competing interests**

562 The authors have declared that they have no competing interests in relation to this study.

563 **Disclaimer**

564 Copernicus Publications remains neutral with regard to jurisdictional claims made in the text, published
565 maps, institutional affiliations, or any other geographical representation in this paper. While Copernicus
566 Publications makes every effort to include appropriate place names, the final responsibility lies with the
567 authors. Views expressed in the text are those of the authors and do not necessarily reflect the views of
568 the publisher.

569 **Acknowledgments**

570 We gratefully acknowledge the invaluable support provided by the members of the Northwest Institute
571 of Eco-Environment and Resources, Chinese Academy of Sciences, Lanzhou, China, during the
572 fieldwork. We would also like to show our gratitude to Dr. Zanpin Xin for meteorological data support.

573 **Financial support**

574 This study was financially supported by the JSPS KAKENHI (25K22868, 24H00260, 22H03731, and
575 21H0457) and Young Scientists Fund of the National Natural Science Foundation of China (42306268
576 and 42201056).

References

Anesio, A.M. and Laybourn-Parry, J.: Glaciers and ice sheets as a biome, Trends Ecol. Evol., 27, 219-225, https://doi.org/10.1016/j.tree.2011.09.012, 2012.

Anesio, A.M., Lutz, S., Chrismas, N.A. and Benning, L.G.: The microbiome of glaciers and ice sheets, npj Biofilms Microbi., 3, 10. https://doi.org/10.1038/s41522-017-0019-0, 2017.

Bradley, J.A., Trivedi, C.B., Winkel, M., Mourot, R., Lutz, S., Larose, C., Keuschnig, C., Doting, E., Halbach, L., Zervas, A. and Anesio, A.M.: Active and dormant microorganisms on glacier surfaces, Geobiol, 21, 244–261, https://doi.org/10.1111/gbi.12535, 2023.

Chen, Y., Takeuchi, N., Tanaka, S. and Li, Z.:. Aggregation of mineral particles in cryoconite granules by multiple species of cyanobacteria on Urumqi Glacier No. 1, China, Front. Earth Sci., 13, 1596472, https://doi.org/10.3389/feart.2025.1596472, 2025.

Cook, J. M., Tedstone, A. J., Williamson, C., McCutcheon, J., Hodson, A. J., Dayal, A., Skiles, M., Hofer, S., Bryant, R., McAree, O. and McGonigle, A.: Glacier algae accelerate melt rates on the south-western Greenland Ice Sheet, The Cryosphere, 14, 309–330, https://doi.org/10.5194/tc-14-309-2020, 2020.

Cook, J., Edwards, A., Takeuchi, N. and Irvine-Fynn, T.: Cryoconite: the dark biological secret of the cryosphere, Prog. Phys. Geog., 40, 66-111, https://doi.org/10.1177/0309133315616574, 2016.

Davey, M.P., Norman, L., Sterk, P., Huete-Ortega, M., Bunbury, F., Loh, B.K.W., Stockton, S., Peck, L.S., Convey, P., Newsham, K.K. and Smith, A.G.: Snow algae communities in Antarctica: metabolic and taxonomic composition, New Phytologist., 222, 1242-1255, https://doi.org/10.1111/nph.15701, 2019.

Di Mauro, B., Garzonio, R., Baccolo, G., Franzetti, A., Pittino, F., Leoni, B., Remias, D., Colombo, R. and Rossini, M.: Glacier algae foster ice-albedo feedback in the European Alps, Sci. Rep., 10, 4739, https://doi.org/10.1038/s41598-020-61762-0, 2020.

Dong, Z., Qin, D., Ren, J., Li, K. and Li, Z., Variations in the equilibrium line altitude of Urumqi Glacier No. 1, Tianshan Mountains, over the past 50 years, Chinese Sci. Bull., 57, 4776-4783, https://doi.org/10.1007/s11434-012-5524-1, 2012.

Hodson, A., Anesio, A.M., Tranter, M., Fountain, A., Osborn, M., Priscu, J., Laybourn-Parry, J. and Sattler, B.: Glacial ecosystems, Ecol. Monogr., 78, 41-67, https://doi.org/10.1890/07-0187.1, 2008.

606 Hodson, A., Cameron, K., Bøggild, C., et al.: The structure, biological activity and biogeochemistry of
607 cryoconite aggregates upon an Arctic valley glacier: Longyearbreen, Svalbard, J. Glaciol., 56, 349–362,
608 https://doi.org/10.3189/002214310791968403, 2010.
609 Hotaling, S., Lutz, S., Dial, R.J., Anesio, A.M., Benning, L.G., Fountain, A.G., Kelley, J.L.,
610 McCutcheon, J., Skiles, S.M., Takeuchi, N. and Hamilton, T.L.: Biological albedo reduction on ice
611 sheets, glaciers, and snowfields. Earth-sci. Rev., 220, 103728,
612 https://doi.org/10.1016/j.earscirev.2021.103728, 2021.
613 Hugonnet, R., McNabb, R., Berthier, E., Menounos, B., Nuth, C., Girod, L., Farinotti, D., Huss, M.,
614 Dussaillant, I., Brun, F. and Kääb, A.: Accelerated global glacier mass loss in the early twenty-first
615 century, Nature, 592, 726-731, https://doi.org/10.1038/s41586-021-03436-z, 2021.
616 Irvine-Fynn, T.D. and Edwards, A.: A frozen asset: the potential of flow cytometry in constraining the
617 glacial biome, Cytom. Part A, 85, 3-7, https://doi.org/10.1002/cyto.a.22411, 2014.
618 Kol, E. and Taylor, W.R.: The snow and ice algae of Alaska, Smithsonian Miscellaneous Collections,
619 101, Smithsonian Institution, 36 pp., 1942.
620 Koshima, S., Seko, K., Yoshimura, Y.: Biotic acceleration of glacier melting in Yala glacier, Langtang
621 region, Nepal Himalaya, IAHS Publ., 218, 309-319, 1993.
622 Langford, H., Hodson, A., Banwart, S. and Bøggild, C.: The microstructure and biogeochemistry of
623 Arctic cryoconite granules, Ann. Glaciol., 51, 87–94, https://doi.org/10.3189/172756411795932083,
624 2010.
625 Li, X., Li, Z., Ding, Y., Liu, S., Zhao, Z., Luo, L., Pang, H., Li, C., Li, H., You, X. and Wang, F.:
626 Seasonal variations of pH and electrical conductivity in a snow-firn pack on Glacier No. 1, eastern
627 Tianshan, China, Cold Reg. Sci. Technol., 48, 55-63, https://doi.org/10.1016/j.coldregions.2006.09.006,
628 2007.
629 Li, Z., Li, H., Dong, Z. and Zhang, M.: Chemical characteristics and environmental significance of
630 fresh snow deposition on Urumqi Glacier No. 1 of Tianshan Mountains, China, Chinese Geogr. Sci., 20,
631 389-397, https://doi.org/10.1007/s11769-010-0412-6, 2010.
632 Ling, H.U. and Seppelt, R.D.: Snow algae of the Windmill Islands, continental Antarctica.
633 Mesotaenium berggrenii (Zygnematales, Chlorophyta) the alga of grey snow, Antarct. Sci., 2, 143-148,
634 https://doi.org/10.1017/s0954102090000189, 1990.

635 Lutz, S., Anesio, A.M., Edwards, A. and Benning, L.G.: Linking microbial diversity and functionality
636 of arctic glacial surface habitats, Enviro. Microbiol., 19, 551-565,
637 https://doi.org/10.1111/1462-2920.13494, 2017.
638 Lutz, S., Anesio, A.M., Raiswell, R., Edwards, A., Newton, R.J., Gill, F. and Benning, L.G.: The
639 biogeography of red snow microbiomes and their role in melting arctic glaciers, Nat. Comm., 7, 11968,
640 https://doi.org/10.1038/ncomms11968, 2016.
641 McCutcheon, J., Lutz, S., Williamson, C., Cook, J.M., Tedstone, A.J., Vanderstraeten, A., Wilson, S.,
642 Stockdale, A., Bonneville, S., Anesio, A.M. and Yallop, M.L.: Mineral phosphorus drives glacier algal
643 blooms on the Greenland Ice Sheet, Nat. Comm., 12, 570, https://doi.org/10.1038/s41467-020-20627-w,
644 2021.
645 Murakami, T., Takeuchi, N., Mori, H., Hirose, Y., Edwards, A., Irvine-Fynn, T., Li, Z., Ishii, S. and
646 Segawa, T.: Metagenomics reveals global-scale contrasts in nitrogen cycling and cyanobacterial
647 light-harvesting mechanisms in glacier cryoconite, Microbiome, 10, 1-14,
648 https://doi.org/10.1186/s40168-022-01238-7, 2022.
649 Musilova, M., Tranter, M., Bamber, J.L., Takeuchi, N. and Anesio, A.M.: Experimental evidence that
650 microbial activity lowers the albedo of glaciers. Geochem, Perspect. Lett., 2, 106-116,
651 https://doi.org/10.7185/geochemlet.1611, 2016.
652 Nagatsuka, N., Takeuchi, N., Nakano, T., Shin, K. and Kokado, E.: Geographical variations in Sr and
653 Nd isotopic ratios of cryoconite on Asian glaciers, Environ. Res. Lett., 9, 045007,
654 https://doi.org/10.1088/1748-9326/9/4/045007, 2014.
655 Oksanen, J., Blanchet, F. G., Kindt, R., Legendre, P., O'hara, R., Simpson, G. L., Solymos, P., Stevens,
656 M. H. H., and Wagner, H.: vegan: Community Ecology Package. R package version 1.17-2,
657 https://cran.r-project.org/web/packages/vegan/index.html, 23, 2010.
658 Onuma, Y., Takeuchi, N., Uetake, J., et al.: Modeling seasonal growth of phototrophs on bare ice on
659 the Qaanaaq Ice Cap, northwestern Greenland, J. Glaciol., 69, 487–499,
660 https://doi.org/10.1017/jog.2022.76, 2023.
661 Ortiz-Álvarez, R., Fierer, N., De Los Ríos, A., Casamayor, E. O., & Barberán, A.: Consistent changes
662 in the taxonomic structure and functional attributes of bacterial communities during primary succession.
663 ISME J, 12(7), 1658-1667, https://doi.org/10.1038/s41396-018-0076-2, 2018.

Remias, D., Holzinger, A., Aigner, S. and Lütz, C.: Ecophysiology and ultrastructure of Ancylonema nordenskiöldii (Zygnematales, Streptophyta), causing brown ice on glaciers in Svalbard (high arctic), Polar Biol., 35, 899-908, https://doi.org/10.1007/s00300-011-1135-6, 2012.

Segawa, T. and Takeuchi, N., Cyanobacterial communities on Qiyi glacier, Qilian Shan, China. Ann. Glaciol., 51, 135-144, https://doi.org/10.3189/172756411795932047, 2010.

Segawa, T., Ishii, S., Ohte, N., Akiyoshi, A., Yamada, A., Maruyama, F., Li, Z., Hongoh, Y. and Takeuchi, N.: The nitrogen cycle in cryoconites: naturally occurring nitrification-denitrification granules on a glacier, Environ. Microbiol., 16, 3250-3262, https://doi.org/10.1111/1462-2920.12543, 2014.

Segawa, T., Matsuzaki, R., Takeuchi, N., Akiyoshi, A., Navarro, F., Sugiyama, S., Yonezawa, T. and Mori, H.: Bipolar dispersal of red-snow algae, Nat. Commun., 9, 3094, https://doi.org/10.1038/s41467-018-05521-w, 2018.

Segawa, T., Takeuchi, N., Mori, H., Rathnayake, R.M., Li, Z., Akiyoshi, A., Satoh, H. and Ishii, S., Redox stratification within cryoconite granules influences the nitrogen cycle on glaciers, FEMS Microbiol. Ecol., 96, fiaa199, https://doi.org/10.1093/femsec/fiaa199, 2020.

Segawa, T., Yonezawa, T., Edwards, A., Akiyoshi, A., Tanaka, S., Uetake, J., Irvine-Fynn, T., Fukui, K., Li, Z. and Takeuchi, N.: Biogeography of cryoconite forming cyanobacteria on polar and Asian glaciers, J. Biogeogr., 44, 2849-2861, https://doi.org/10.1111/jbi.13089, 2017.

Segawa, T., Yonezawa, T., Matsuzaki, R., Mori, H., Akiyoshi, A., Navarro, F., Fujita, K., Aizen, V.B., Li, Z., Mano, S. and Takeuchi, N.: Evolution of snow algae, from cosmopolitans to endemics, revealed by DNA analysis of ancient ice, ISME J., 17, 491-501, https://doi.org/10.1038/s41396-023-01359-3, 2023.

Singh, P., Kumar, N. and Pal, S.: Chapter 10 - Cyanobacteria in the polar regions: diversity, adaptation, and taxonomic problems, Understanding Present and Past Arctic Environments, 189-212, ISBN 9780128228692, https://doi.org/10.1016/B978-0-12-822869-2.00013-X，2021.

Stibal, M. and Tranter, M.: Laboratory investigation of inorganic carbon uptake by cryoconite debris from Werenskioldbreen, Svalbard, J. Geophys. Res-Biogeo., 112, https://doi.org/10.1029/2007JG000429, 2007.

692 Stibal, M., Box, J. E., Cameron, K. A., Langen, P. L., Yallop, M. L., Mottram, R. H., et al.: Algae drive
693 enhanced darkening of bare ice on the Greenland ice sheet, Geophys. Res. Lett., 44, 11,463–11,471,
694 https://doi.org/10.1002/2017GL075958, 2017.
695 Stibal, M., Šabacká, M. and Žárský, J.: Biological processes on glacier and ice sheet surfaces, Nat.
696 Geosci., 5, 771-774, https://doi.org/10.1038/ngeo1611, 2012a.
697 Stibal, M., Telling, J., Cook, J., Mak, K.M., Hodson, A. and Anesio, A.M.: Environmental controls on
698 microbial abundance and activity on the Greenland ice sheet: a multivariate analysis approach, Micro.
699 Ecol., 63, 74-84. https://doi.org/10.1007/s00248-011-9935-3, 2012b.
700 Takeuchi, N. and Kohshima, S.: A snow algal community on Tyndall Glacier in the Southern Patagonia
701 Icefield, Chile, Arct. Antarct. Alp. Res., 36, 92–99,
702 https://doi.org/10.1657/1523-0430(2004)036[0092:ASACOT]2.0.CO;2, 2004.
703 Takeuchi, N. and Li, Z.: Characteristics of surface dust on Ürümqi glacier No. 1 in the Tien Shan
704 mountains, China, Arct. Antarct. Alp. Res., 40, 744-750,
705 https://doi.org/10.1657/1523-0430(07-094)[takeuchi]2.0.co;2, 2008.
706 Takeuchi, N., Ishida, Y. and Li, Z.: Microscopic analyses of insoluble particles in an ice core of
707 Ürümqi Glacier No. 1: Quantification of mineral and organic particles, J. Earth Sci., 22, 431-440,
708 https://doi.org/10.1007/s12583-011-0197-2, 2011.
709 Takeuchi, N., Nishiyama, H. and Li, Z.: Structure and formation process of cryoconite granules on
710 Ürümqi Glacier No. 1, Tien Shan, China, Ann. Glaciol., 51, 9–14,
711 https://doi.org/10.3189/172756411795932010, 2010.
712 Takeuchi, N., Sakaki, R., Uetake, J., Nagatsuka, N., Shimada, R., Niwano, M. and Aoki, T.: Temporal
713 variations of cryoconite holes and cryoconite coverage on the ablation ice surface of Qaanaaq Glacier
714 in northwest Greenland, Ann. Glaciol., 59, 21-30, https://doi.org/10.1017/aog.2018.19, 2018.
715 Takeuchi, N., Tanaka, S., Konno, Y., Irvine-Fynn, T.D., Rassner, S.M. and Edwards, A.: Variations in
716 phototroph communities on the ablating bare-ice surface of glaciers on Brøggerhalvøya, Svalbard,
717 Front. Earth Sci., 7, 4, https://doi.org/10.3389/feart.2019.00004, 2019.
718 Takeuchi, N., Uetake, J., Fujita, K., Aizen, V.B. and Nikitin, S.D.: A snow algal community on Akkem
719 glacier in the Russian Altai mountains, Ann. Glaciology, 43, 378-384,
720 https://doi.org/10.3189/172756406781812113, 2006.

721 Takeuchi, N.: Optical characteristics of cryoconite (surface dust) on glaciers: the relationship between
722 light absorbency and the property of organic matter contained in the cryoconite, Ann. Glaciology, 34,
723 409-414, https://doi.org/10.3189/172756402781817743, 2002.
724 Takeuchi, N.: Seasonal and altitudinal variations in snow algal communities on an Alaskan glacier
725 (Gulkana glacier in the Alaska range), Environ. Res. Lett., 8, 035002,
726 https://doi.org/10.1088/1748-9326/8/3/035002, 2013.
727 Takeuchi, N.: Temporal and spatial variations in spectral reflectance and characteristics of surface dust
728 on Gulkana Glacier, Alaska Range, J. Glaciol., 55, 701–709,
729 https://doi.org/10.3189/002214309789470914, 2009.
730 Takeuchi, N.: The altitudinal distribution of snow algae on an Alaska glacier (Gulkana Glacier in the
731 Alaska Range), Hydrol. Process., 15, 3447-3459, https://doi.org/10.1002/hyp.1040, 2001.
732 Uetake, J., Naganuma, T., Hebsgaard, M.B., Kanda, H. and Kohshima, S.: Communities of algae and
733 cyanobacteria on glaciers in west Greenland, Polar Sci., 4, pp.71-80,
734 https://doi.org/10.1016/j.polar.2010.03.002, 2010.
735 Uetake, J., Nagatsuka, N., Onuma, Y., Takeuchi, N., Motoyama, H. and Aoki, T.: Bacterial community
736 changes with granule size in cryoconite and their susceptibility to exogenous nutrients on NW
737 Greenland glaciers, FEMS Microbiol. Ecol., 95, fiz075, https://doi.org/10.1093/femsec/fiz075, 2019.
738 Williamson, C.J., Anesio, A.M., Cook, J., Tedstone, A., Poniecka, E., Holland, A., Fagan, D., Tranter,
739 M. and Yallop, M.L.: Ice algal bloom development on the surface of the Greenland Ice Sheet, FEMS
740 Microbiol. Ecol., 94, fiy025, https://doi.org/10.1093/femsec/fiy025, 2018.
741 Wu, G., Zhang, C., Li, Z., Zhang, X. and Gao, S.: Iron content and solubility in dust from high-alpine
742 snow along a north-south transect of High Asia, Tellus B, 64, 17735,
743 https://doi.org/10.3402/tellusb.v64i0.17735, 2012.
744 Yallop, M.L., Anesio, A.M., Perkins, R.G., Cook, J., Telling, J., Fagan, D., MacFarlane, J., Stibal, M.,
745 Barker, G., Bellas, C. and Hodson, A.: Photophysiology and albedo-changing potential of the ice algal
746 community on the surface of the Greenland ice sheet, ISME J., 6, 2302-2313,
747 https://doi.org/10.1038/ismej.2012.107, 2012.
748 Ye, B., Yang, D., Jiao, K., Han, T., Jin, Z., Yang, H. and Li, Z.: The Urumqi River source glacier No. 1,
749 Tianshan, China: changes over the past 45 years, Geophys. Res. Lett., 32,
750 https://doi.org/10.1029/2005gl024178, 2005.

751 Yoshimura, Y., Kohshima, S. and Ohtani, S.: A community of snow algae on a Himalayan glacier:
752 change of algal biomass and community structure with altitude, Arct. Antarct. Alp. Res., 29, 126-137,
753 https://doi.org/10.1080/00040851.1997.12003222, 1997.
754 Yue, X., Li, Z., Li, H., Wang, F. and Jin, S.: Multi-temporal variations in surface albedo on Urumqi
755 Glacier No. 1 in Tien Shan under arid and semi-arid environment, Remote Sens., 14, 808,
756 https://doi.org/10.3390/rs14040808, 2022.
757